IEEE Access
Multidisciplinary ⋮ Rapid Review ⋮ Open Access Journal

Received 4 September 2024, accepted 4 October 2024, date of publication 10 October 2024, date of current version 21 October 2024.

Digital Object Identifier 10.1109/ACCESS.2024.3477974

RESEARCH ARTICLE

Can Stochastic Resonance Improve Sensorimotor Performance in Hand Motor Control?

MICHELE POMPILIO[1,2], (Member, IEEE), NICOLE D'AURIZIO[1,2], (Member, IEEE), TOMMASO LISINI BALDI[1,2], (Member, IEEE), GIONATA SALVIETTI[1,2], (Senior Member, IEEE), SIMONE ROSSI[3], AND DOMENICO PRATTICHIZZO[1,2], (Fellow, IEEE)

[1]Department of Information Engineering and Mathematics, University of Siena, 53100 Siena, Italy
[2]Humanoids and Human Centered Mechatronics Centre, Istituto Italiano di Tecnologia, 16163 Genoa, Italy
[3]Department of Medicine, Surgery and Neuroscience, University of Siena, 53100 Siena, Italy

Corresponding author: Tommaso Lisini Baldi (tommaso.lisini@unisi.it)

This work was supported in part by European Union's Horizon Europe Programme of the project "HARIA—Human-Robot Sensorimotor Augmentation—Wearable Sensorimotor Interfaces and Supernumerary Robotic Limbs for Humans with Upper-Limb Disabilities" from the Next Generation EU Project "Ecosistema dell'Innovazione" Tuscany Health Ecosystem (THE) (PNRR, Spoke 9: Robotics and Automation for Health) under Project 101070292 and Project ECS00000017; and in part by the University of Siena Curiosity Driven (F-CUR) Project "BRIOCHE: wearaBle sensoRImOtor interfaCes for Human augmentation.

ABSTRACT Recent researches have demonstrated that noise, whether mechanical or electrical, can enhance somatosensation and optimize balance control in humans. However, the influence of stochastic resonance (SR) on the human motor system, particularly regarding hand motor control, remains largely unexplored. This study examines the impact of stochastic resonance on enhancing sensorimotor performance in the human motor system, specifically in the context of hand motor control when tools are held. While many of the previous studies have focused on SR in free-hand motions, few studies have examined the effects when tools are adopted. Our experimental campaign involved forty participants who were asked to track a given trajectory displayed in mixed reality while holding various tools. The experiment considered four subthreshold levels of vibratory mechanical noise, three hand stimulation sites with three different haptic interfaces, and three distinct 3D trajectories. Results indicate that wearing a device typically degrades performance in trajectory tracking. However, when SR is applied, the precision of hand motor control is restored to levels comparable to those observed without any devices. These findings suggest that SR can mitigate the negative impact of holding tools on sensorimotor precision.

INDEX TERMS Haptics, wearable haptics, mixed reality, human performance augmentation.

I. INTRODUCTION

Over the past few years, studies have demonstrated how noise can be employed to improve the detection and transmission of weak signals within specific nonlinear systems, utilizing a mechanism known as stochastic resonance (SR) [1]. Examples of successful use of SR range from physics and engineering to biology and medicine, including electronic circuits [2] and sensory information processes [3]. For instance, the phenomenon of stochastic resonance has been both experimentally and theoretically investigated in state-of-the-art metal-oxide memristive devices. The findings indicate that noise and fluctuations can play a constructive role in nonlinear memristive systems far from equilibrium [4]. In [5] and [6], the authors studied the effects of vibration stimulation on the overall performance of motor imagery paradigms. Similarly, Monifi et al. [7] reported the phenomenon of chaos-induced stochastic resonance in an optomechanical system, which could potentially enhance the detection of otherwise undetectable signals in such systems. Qiao and Shu [8] investigated how noise can be leveraged in coupled neurons to amplify weak signals embedded within noisy

The associate editor coordinating the review of this manuscript and approving it for publication was Lei Wei.

environments, subsequently applying their insights to improve the detection of weak fault signatures in mechanical fault diagnosis. Drawing inspiration from nonlinear dynamics in biophysics, numerous researchers have focused on uncovering the benefits of noise in biological systems. Mitaim and Kosko [9] demonstrated that SR in neurons remains robust against significant noise variations, thereby improving the mutual information between input and output. Blanchard et al. [10] explored the advantages of noise in parallel arrays of nonlinear neurons with thresholds and saturation, specifically for signal transduction. Hänggi [1] illustrated how noise can enhance the detection of weak useful signals and improve biological information processing.

In humans, the phenomenon of stochastic resonance allows for the utilization of input noise, whether mechanical or electrical, to enhance the performance of the balance control system [11]. For instance, in [12] the authors show for the first time that an individually measured optimal level of mechanical Gaussian noise can improve the performance in a visuomotor task requiring an isometric force compensation by the index fingers. Germer et al. [13] experimentally verified that an optimal level of vibration can improve force steadiness, accounting for the enhancement in force control. Similarly in [14], the authors investigated the inherent characteristics of neural-muscular activity during dynamic hand strength adjustment.

The main rationale behind this effect lies in the fact that SR lowers the threshold at which mechanoreceptors perceive stimuli and reduces postural sway [15]. For instance, the reduction of body oscillations that occurs when individuals maintain contact between a finger and a stable surface [16], [17] can be further decreased by the application of vibratory noise to the point of touch [18], and the influence of SR on the frequency components of body sway appears to depend on the relative amplitude of the vibratory stimulus [19]. Vibrotactile stimulation of the index finger can also lead to improvements in sensorimotor performance during a visuomotor task, in alignment with the observed increase in cortical motor spectral power and in corticomuscular coherence [20]. In a study conducted by Lee et al. [21], noisy galvanic vestibular stimulation was applied to subjects affected by Parkinson's disease while they were engaged in a sinusoidal visuomotor joystick tracking task. Results showed a notable enhancement of their motor performance. Moreover, imperceptible levels of SR applied to the vestibular system have demonstrated to enhance ocular stabilization reflexes in response to whole-body tilt, and to improve postural balance performance in Parkinson's patients [22].

These findings have been expanded through investigations into specific levels of mechanical noise applied to various body parts. For instance, Mendez-Balbuena et al. [23] explored the application of particular levels of mechanical Gaussian noise (ranging from 0 to 15 Hz) to the index finger. Results showed an enhancement of performance in compensating for

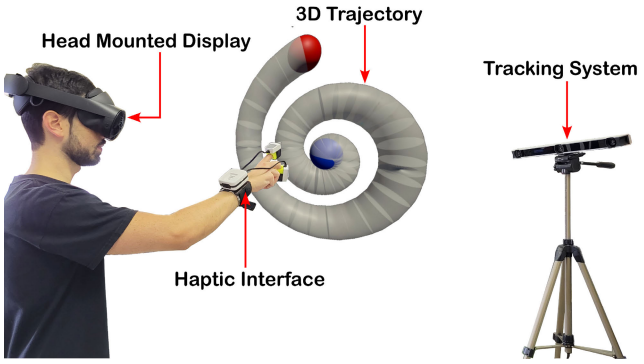

FIGURE 1. Experimental setup. The subject wears an head mounted display that renders a 3D trajectory within a mixed reality environment. The user has to follow the path by using their hand while wearing a haptic interface delivering subthreshold vibratory mechanical noise. The tracking system captures their hand movements.

a static force generated by a manipulandum when the noise level inducing SR varied between 0 and 200 mN. In [24], the application of subthreshold vibratory noise to the subjects' dominant upper arms and forearms improved performance in terms of accuracy and speed in a simulated laparoscopic palpation task. Wells et al. [25] demonstrated that subthreshold vibratory noise stimulation effectively heightened plantar sensitivity. A systematic review [26] on the advantages of subthreshold vibratory noise stimulation applied to the soles of the feet revealed compelling evidence supporting the enhancement of balance and gait performance in both older adults and individuals with diabetes. These results suggest the importance of fine-tuning the stimulation parameters to align with the unique needs of each individual.

While the advantages of SR concerning muscle proprioception and tactile sensitivity perception are well-documented in literature, there remains a notable gap in comprehensive studies that explore its potential benefits related to human hand movements. Recent studies have studied the influence of SR on visuomotor temporal integration and hand motor function, aiming to explore the potential utility of SR as a neurorehabilitation tool. In a study conducted by Nobusako et al. [27], the authors successfully demonstrated how the use of vibrotactile noise (white noise signal low-pass filtered at 500 Hz) applied to the wrist efficiently improves the visuomotor temporal integration. However, their study did not conclusively establish whether SR can also enhance human hand motion performance. A preliminary exploration of the impact of SR on the balance control of human hand movements was undertaken by Duan et al. [28], where they investigated the effects of mechanical vibration generated by micro-motors. However, their study was limited to a two-dimensional tracking task in which participants were required to follow a straight line on a blackboard by using a laser pointer. Additionally, their work was a preliminary research report lacking a discussion on the results and a detailed description of the parameters employed, including the noise levels used.

Taking these considerations into account, this study proposes to further investigate the influence of SR on the control of hand movements by analyzing users performance in a more comprehensive three-dimensional tracking task where also hand-held tools are considered. In literature it has been demonstrated that SR can enhance sensorimotor capabilities also when a certain tool is grasped by the user [29]. However, to the best of our knowledge, no studies have focused on the enhancement of the precision of the hand in tracking a certain trajectory while holding a tool. To this aim, we take into account various subthreshold vibratory mechanical noise levels, different hand sites for stimulation, and multiple 3D trajectories. Two commercially-available devices were adopted within the study. This allowed us to assess the influence of held object on trajectory tracking performance (e.g., because of factors such as device weight, encumbrance, and ergonomics) compared to when the tracking task is executed using the bare hand, and whether SR can potentially mitigate or even reverse this effect.

This study is beneficial to multiple fields of application. For instance, its findings can be instrumental in scenarios involving the design of innovative interfaces, thereby aiding in the decision-making process regarding the adoption or customization of specific controllers. Moreover, the outcomes of this research could be crucial in enhancing user tracking capabilities, thereby contributing to the development of novel technologies aimed at improving human performance across various domains. This is particularly relevant in fields where precise hand motion while manipulating instruments for specific tasks is of utmost importance, from industrial applications to surgical procedures. As an example, the application of vibrotactile noise to a welding gun holds the potential to assist manual welders in maintaining precision during welding tasks, where the accurate fusion of pieces is essential. Similarly, applying stochastic resonance to surgical instruments could aid surgeons in achieving precision while cutting or suturing during surgical operations.

The rest of the paper is organized as follows. The next section (Section II) provides a detailed description of the system. Section III presents the experimental validation, while the corresponding results are discussed in Section IV. Finally, Section V outlines the conclusions and suggests directions for future work.

II. SYSTEM DESCRIPTION

A Mixed Reality (MR) environment based on the Unity 3D engine was developed for the purpose of this work. Participants were asked to move a virtual cursor to follow a 3D virtual path placed in front of them, within their real surrounding environment (see Fig. 1). Three haptic interfaces were used for delivering subthreshold vibrotactile white noise to specific locations on the users' hand. Depending on the experimental condition, a tracking system accurately acquired either the position of the index finger or that of the device, which was then translated into the position of the virtual cursor.

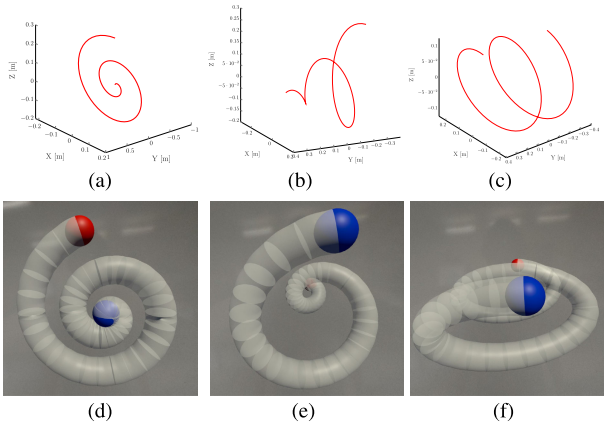

FIGURE 2. 3D trajectories used for the purposes of this study. In a), b), and c), the points generated through Matlab for the planar circular spiral, the circular conical helix, and the elliptical cylindrical helix, respectively. The corresponding 3D meshes displayed within the mixed reality environment are in d), e), and f). For each 3D path, the starting position is highlighted with a blue sphere, while the ending position is depicted with a red sphere.

In the following sections, we provide a detailed description of the system components, including the MR environment for displaying 3D paths, the haptic interfaces, the tracking system, and the calibration procedures.

A. MIXED REALITY ENVIRONMENT AND 3D VIRTUAL PATHS

To effectively design a 3D tracking task, we selected the three 3D virtual paths adopted in [30] to demonstrate that human hand movements are inherently three-dimensional and not a concatenation of two-dimensional planar segments. More in detail, the trajectories were: *i)* a planar circular spiral, *ii)* a circular conical helix, and *iii)* an elliptical cylindrical helix. The corresponding path points, depicted in Fig. 2a, Fig. 2b, and Fig. 2c, were generated in Matlab (The MathWorks Inc., US) using the following equations:

$$\mathcal{S}: \begin{bmatrix} X_s \\ Y_s \\ Z_s \end{bmatrix} = \begin{bmatrix} R\alpha(t_n)cos(t_n) \\ R\alpha(t_n)sin(t_n) \\ 0 \end{bmatrix}$$

$$\mathcal{C}: \begin{bmatrix} X_c \\ Y_c \\ Z_c \end{bmatrix} = \begin{bmatrix} R\alpha(t_n)cos(t_n) \\ R\alpha(t_n)sin(t_n) \\ 0.3-vt_n \end{bmatrix}$$

$$\mathcal{E}: \begin{bmatrix} X_e \\ Y_e \\ Z_e \end{bmatrix} = \begin{bmatrix} R_x\alpha(t_n)cos(t_n) \\ R_y\alpha(t_n)sin(t_n) \\ 0.3-vt_n \end{bmatrix}$$

with

$$\alpha(t_n)=\frac{t_n}{4\pi}, \quad t_n=n\frac{t}{N}, \quad n=[0,1,\ldots,N], \quad 0\le t\le 4\pi$$

where $\mathcal{S}$ is the set of points describing the spiral, $\mathcal{C}$ is the set of points describing the cone, $\mathcal{E}$ is the set of points describing the ellipse, $R = 0.25$ m, $R_x = 0.125$ m, $R_y = 0.25$ m, and

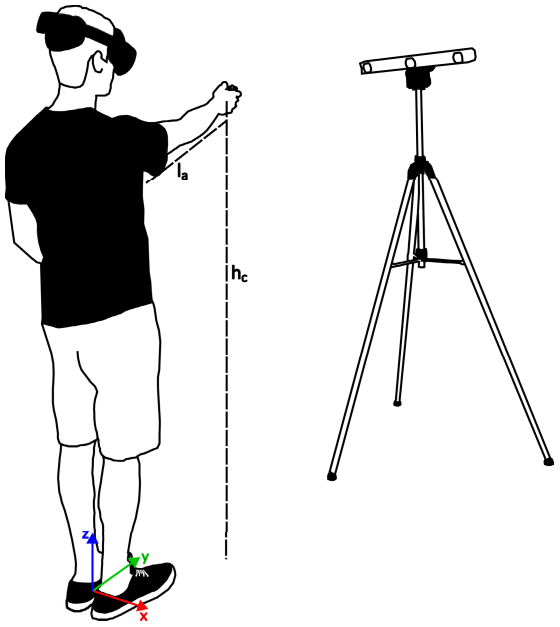

FIGURE 3. Schematic overview of the experimental setup. Before the starting of the experiment, participants received specific instructions to stand in front of the tracking system, extend their arm forward to align the Quest Pro controller with the height of their chin, and press a controller button. The system recorded the user's chin height h_c and the user's arm length l_a to scale and position the path for the experiment. The reference frame of the mixed reality environment is anchored at the user's feet.

$v = 0.6/4\pi$. For each path, the equations generate a point cloud consisting of $N = 100$ points.

The three point clouds were rendered in MR via an Oculus Meta Quest Pro (Meta, USA) as 3D meshes of cylinders having radius $r = 0.04$ m (see Fig. 2d-f). Consequently, all trajectories appeared to users as 3D tubular paths, including the spiral (Fig. 2a), which inherently consisted of points in a 2D plane. Thus, users were consistently tasked with maintaining precise alignment along all three dimensions to stay within the confines of the tubular path.

The reference frame in the MR environment was centered at the user's feet with the x-axis perpendicular to the sagittal plane pointing to the right, the y-axis perpendicular to the frontal plane pointing forward, and the z-axis perpendicular to the transverse plane pointing upward (see Fig. 3). By exploiting the Meta Quest Pro pass-through function, users were able to see both the real surrounding environment and the 3D virtual shapes. Mixed reality was chosen over virtual reality primarily because of the task's requirement of tracking a trajectory with one's hand. The ability to perceive the real surrounding environment is crucial for enhancing users' proprioception of body movements, particularly those related to the hand, a feature that cannot be achieved in a purely virtual environment as shown by Bayramova et al. in [31].

Path Calibration: For positioning and scaling the paths considering the users' arm position and length, we implemented a calibration procedure. Before the start of the experiment, each participant received specific instructions to extend their arm forward and align the Quest Pro controller with the height of their chin. Then, when the user clicked a controller button, the system recorded both the user's chin height h_c and the user's arm length l_a, computed as the difference between the controller position and the position of the Head-Mounted Display (HMD) along the z- and y- axis, respectively. This allowed to position and scale each 3D path in the MR environment according to:

$$\hat{X}_i(t) = x_{HMD}(t) + \alpha X_i$$
$$\hat{Y}_i(t) = y_{HMD}(t) + 0.7\, l_a + \alpha Y_i$$
$$\hat{Z}_i(t) = z_{HMD}(t) - h_c + \alpha Z_i$$
$$\alpha = 0.5 \frac{l_a}{y_i(n) - y_i(1)}$$

where t is the current time instant, $\hat{X}_i(t), \hat{Y}_i(t), \hat{Z}_i(t)$ are the 3D coordinates of the path P_i for $i = \{s, c, e\}$, $x_{HMD}(t), y_{HMD}(t), z_{HMD}(t)$ represent the HMD position expressed in MR environment reference frame, X_i, Y_i, Z_i are the set of points defining the path P_i, $y_i(n), y_i(1) \in Y_i$ represent the minimum and the maximum points of the path P_i along the y-axis (with their difference being the size of the shape along the y-axis), and α is the scaling factor. As a result, the center of each shape was anchored in the MR space at a height equal to the user's chin height, maintaining a distance along the y-axis equal to 70% of the user's arm length, and then scaled so that its depth matched the 50% of the user's arm length. The same scaling factor was used to compute the radius of the 3D mesh corresponding to the path, i.e. $\hat{r} = \alpha r$. We decided to place the paths in a fixed position with respect to the user's head to encourage subjects to interact with the virtual shapes using their hand, rather than relying on body movements within the space. Additionally, calibrating each trajectory to the specific body measurements of individual subjects introduced variability in the trajectories throughout the entire experimental campaign.

B. HAPTIC INTERFACES AND VIBROTACTILE WHITE NOISE

White noise low-pass filtered at 500 Hz [27] was delivered in the form of mechanical vibration through three different haptic interfaces (Fig. 4), of which two were commercial devices and one was a custom-made system. The first commercial device was the TouchDiver (Weart, IT) (see Fig. 4a), a haptic glove able to provide vibrotactile stimuli at the thumb, index and middle fingertips, with a frequency range from 20 Hz to 500 Hz, and a weight of 252 g. During the experiments, the vibration was applied only at the index fingertip. The second commercial device was the Meta Quest Pro controller (see Fig. 4b), which is able to provide mechanical vibrations with a frequency range from 50 Hz to 500 Hz to the whole hand, and weights 163 g. The last haptic interface was an arm support with gravity compensation (SaeboMAS, Saebo, US) with a voice coil (vibro-transducer Vp210, Acouve Laboratory, Inc., JP) attached in correspondance of the wrist location (see Fig. 4c). The voice coil has an operational frequency

range of $20-15000$Hz, and was driven by an audio amplifier (LepaiLP2020A+, Parts Express, US).

Depending on the experimental condition, the desired vibrotactile signal was generated in real-time, filtered, and wirelessly transmitted by the Meta Quest Pro to the haptic interface in use.

Subthreshold Level Calibration: To determine the subthreshold vibratory mechanical noise levels, we implemented a calibration procedure using a custom-designed descending staircase method [32]. The minimum vibration intensity perceived by the subject was assessed by cyclically repeating the following three phases:

Evaluation: a vibrotactile signal lasting 3 s was given to the subject through their assigned haptic interface;

Interview: the subject was asked about their perception of the haptic signal, specifically whether they felt any vibration on their hand (with possible responses being "Yes" or "No");

Update: the vibration intensity $\hat{I}_v$ was adjusted based on the subject response. This adjustment followed a staircase progression with a dynamic step size, calculated as:

$$\hat{I}_v(k) = \hat{I}_v(k-1) + \eta(k)\Delta(k)$$
$$\Delta(k) = \beta(k)\Delta(k-1)$$

where $\Delta(k)$ represents the step size at the current iteration k, $\Delta(k-1)$ is the step size applied at the previous iteration $k-1$, and β is the step size scaling factor. The value of $\eta(k)$ and $\beta(k)$ changed based on the user answer $a(k)$ as follows:

$$\eta(k) = \begin{cases} 1 & \text{if } a(k) = \text{"No"}, \\ -1 & \text{if } a(k) = \text{"Yes"}; \end{cases}$$

$$\beta(k) = \begin{cases} 1 & \text{if } a(k) = a(k-1), \\ 0.75 & \text{if } a(k) \neq a(k-1). \end{cases}$$

This three-phase procedure was repeated until the user changed their answer three times consecutively. From that point, the procedure continued for other 5 iterations and then stopped. The sensory threshold level I_v was calculated as the mean value of the last 5 vibration intensities.

C. TRACKING SYSTEM

To accurately track the user's hand position, passive retroreflective markers were placed as close as possible to the user hand according to the haptic interface in use. In particular, for the TouchDiver, the retroreflective marker was attached to the index thimble of the device (Fig. 4a). For the Quest Pro controller, the marker was positioned on top of the device (Fig. 4b). In the case of the the arm gravity compensator with the voice coil, the marker was mounted on an ABS ring designed to be worn on the user's index finger (Fig. 4c). Users who performed the tracking task without any haptic interface exclusively wore the ABS ring with the retroreflective marker on their index finger. The 3D position of these markers was measured with an OptiTrack V120:Trio system (NaturalPoints, Inc., US) at a sample rate of 120 Hz and with a sub-millimiter accuracy in all dimensions. The OptiTrack three-dimensional coordinate system was set up to coincide with the Quest Pro virtual world reference frame. As a result, users could interact with the virtual shapes using a virtual spherical cursor with radius $r_c = 0.015$ m. To ensure precise alignment between the virtual cursor and the passive marker, we refrained from scaling the virtual cursor according to the path scaling. This decision was made to maintain a consistent aspect ratio between the real object (the marker) and the virtual object (the cursor).

III. EXPERIMENTAL EVALUATION

The goal of the experimental campaign was to assess whether vibratory mechanical subthreshold SR applied at the hand improves precision in 3D path tracking. Forty subjects were involved in the evaluation. Each subject gave their written informed consent to participate and was able to discontinue participation at any time during experiments. The experimental evaluation protocols followed the Declaration of Helsinki, and there was no risk of harmful effects on subjects' health. We evaluated three distinct scenarios concerning the location at which the vibration was applied on the hand. For this reason, participants were divided into four groups (10 participants per group):

Group 1 - TouchDiver: (5 males, 5 females, age 19-26y, all right-handed) SR applied at the index fingertip using the TouchDiver. Path tracking is performed using the index finger;

Group 2 - QuestPro: (6 males, 4 females, age 25-30y, all right-handed) SR applied at the palm using the Quest Pro controller. Path tracking is performed using the controller as a pointing device;

Group 3 - VoiceCoil: (5 males, 5 females, age 22-36y, all right-handed) SR applied at the wrist using the arm support embedding the voice coil. Path tracking is performed using the index finger;

Group 4 - Control: (4 males, 6 females, age 21-30y, all right-handed) control group, subjects performed the experiment with no devices, hence no SR applied. Path tracking is performed using the index finger.

According to [33], task performance can be enhanced by applying noise with an intensity below the subthreshold value. Hence, we decided to analyze SR effects at three different noise intensities, i.e. 40%, 60%, and 80% of the sensory threshold level. Additionally, we included a control condition at 0% in which no SR was applied. As a result, each participant performed 36 trials, given by the combination of 3 paths ($\mathcal{S}$, $\mathcal{C}$, and $\mathcal{E}$, see Sect. II-A) with 4 subthreshold levels ($I_{0\%} = 0$, $I_{40\%} = 0.4I_v$, $I_{60\%} = 0.6I_v$, and $I_{80\%} = 0.8I_v$, see Sect. II-B). Each combination was presented three times, delivered in a pseudo-randomized sequence. Participants in the Control group underwent an equivalent number of trials, however no stimulation was provided in their case as they did not have a device.

(a) (b) (c)

FIGURE 4. The devices used to provide subthreshold vibratory mechanical noise. In a), the TouchDiver, in b), the Quest Pro controller, and in c), the arm support with a voice coil mounted at the wrist (highlighted with a blue dashed circle). The red dashed circles highlight how passive retroreflective markers are positioned for each haptic interface.

At the beginning of the experimental session, participants were asked to stand in front of the tracking system, and wear the HMD along with a pair of headsets and the haptic interface corresponding to their assigned group. White noise was provided by means of the headsets throughout the session to mask environmental sounds and noise generated by the setup. Then, each user was asked to perform two calibration procedures, i.e. one to calibrate the subthreshold levels using the procedure detailed in Sect. II-B, and one to calibrate the MR environment using the procedure detailed in Sect. II-A. All subjects reported that they did not feel the vibratory mechanical subthreshold SR during the experiment.

In each trial, the task required controlling the virtual cursor (see Sect. II-C) to track as quick and accurate as possible the proposed 3D path, starting from the red sphere and ending at the blue one (see Fig. 2).

Performance Metrics: Subject performance was measured by computing for each trial *i)* translational path error (TPE), *ii)* trial time (TT), and *iii)* combined translational path error multiplied by trial time (CET). Following [34], TPE was calculated as:

$$TPE = \sum_{j=1}^{J} \varphi_j \|\boldsymbol{p}_{j,act} - \boldsymbol{p}_{j,des}\| \|\boldsymbol{p}_{j-1,des} - \boldsymbol{p}_{j,des}\|$$

where J is the number of samples acquired for the trial, with $j = 1$ being the first sample within the starting position and $j = J$ being the last sample within the ending position, $\boldsymbol{p}_{j,act}$ is the j-th sample of the user trajectory, and $\boldsymbol{p}_{j,des}$ is the closest point on the desired trajectory (i.e., the 3D path). The term φ_j penalizes the performance when the virtual cursor is outside the 3D virtual object, and is defined as:

$$\varphi_j = \begin{cases} 10 & \text{if } \|\boldsymbol{p}_{j,act} - \boldsymbol{p}_{j,des}\| > \hat{r}; \\ 1 & \text{otherwise.} \end{cases}$$

For the purposes of the analysis, the three point clouds $\mathcal{S}$, $\mathcal{C}$, and $\mathcal{E}$ were upsampled to increase the number of points from 100 to 5000. This was done to ensure that the closest point on the desired trajectory was as accurate as possible. As regards trial time, it was measured from the time instant in which the virtual cursor entered the red sphere until it reached the blue one. Finally, trial CET was computed as:

$$CET = TPE \cdot TT.$$

This resulting metric considers the speed-accuracy tradeoff as an overall measure of performance [35]. It emphasizes the need of maintaining precision while minimizing time in the tracking task.

IV. RESULTS

Collected data were statistically analized to assess differences in performance under the different experimental conditions. A three-way between-within-within mixed ANOVA, with one between-subjects and two within-subjects factors, was run to understand the effects of different devices, subthreshold levels, and trajectories on CET, TPE and TT when users were asked to accomplish a 3D tracking task. Trajectory and subthreshold were within-subjects effects, while device was the between-subjects effect. A total of 1440 values for each metric was collected during the experimental campaign, with each of the 40 participants performing the task with 3 trajectories and 4 different subthreshold levels, each repeated 3 times. For the analysis, we averaged the performance of the three trials, resulting in 480 values for index. In what follow, we present and discuss the results of each metric.

A. COMBINED ERROR-TIME (CET)

1) PRELIMINARY STATISTICAL ANALYSIS

As a first step, we started considering CET values. The mean CETs obtained were not initially normally distributed, as assessed by Shapiro-Wilk's test (data were moderately positively skewed to normality), thus logaritmic transformation was applied [36]. After that, all the data were normally distributed ($p > 0.05$). There were four outliers, as confirmed by boxplot inspection. The outliers were removed from the analysis because they did not materially affect the results, as assessed by comparing the results with and without the outliers. There was homogeneity of variances among the groups, as confirmed by Levene's test for equality of variances ($p > 0.05$). The group sample sizes were approximately equal, and the ratio of the largest group variance (1.39) to the smallest group variance (0.55) was 2.53, thus less than 3. Such condition allowed to run the three-way mixed ANOVA

anyway because this test is robust to heterogeneity of variance in these circumstances [37].

For the three-way interaction effect, Mauchly's test of sphericity indicated that the assumption of sphericity was violated. Consequently, a Greenhouse-Geisser correction was applied. The test revealed no statistically significant three-way interaction between device, trajectory and subthreshold, $F(13.38, 147.13) = 1.057$, $p = 0.401$. However, a statistically significant two-way interaction was assessed between subthreshold and device, $F(6.69, 73.63) = 2.854$, $p = 0.012$. Conversely, there were no statistically significant two-way interactions between trajectory and device ($F(5.73, 62.98) = 0.856$, $p = 0.528$), and trajectory and subthreshold ($F(4.46, 147.13) = 0.85$, $p = 0.506$). Even though trajectory showed no statistically significant interaction with device and subthreshold, its main effect revealed a statistically significant difference in CET values between the different trajectories proposed ($F(1.91, 62.98) = 58.851$, $p < 0.001$). This confirms that, although different trajectories influence CET due to varying difficulty levels, the impact of subthreshold vibratory noise and device on performance is independent of the difficulty of the trajectory.

2) INTERACTION BETWEEN CET AND SUBTHRESHOLD

Building upon the results of the test, we decided to conduct a more thorough investigation into the interaction between subthreshold and CET considering the effect of the device. This was done by further exploring the two-way interaction showed by the ANOVA. The simple main effect of device on CET was investigated at each subthreshold level by running a one-way model. The results demonstrated that the simple main effect of the device was significant for each subthreshold level ($p < 0.001$). Multiple pairwise comparison through estimated marginal means (EMMs) method were conducted, to determine which device effects were statistically significant at each subthreshold level. More in detail, scored CETs were statistically significantly different in the following conditions ($p < 0.05$):

- $I_{0\%}$: Control outperform VoiceCoil and TouchDiver. QuestPro is better than VoiceCoil;
- $I_{40\%}$: TouchDiver, QuestPro, and Control are better than VoiceCoil;
- $I_{60\%}$: QuestPro and Control are better than VoiceCoil;
- $I_{80\%}$: TouchDiver, QuestPro, and Control are better than VoiceCoil.

In Fig. 5 we visually summarize the statistical differences between groups within each subthreshold. These results suggest that the subthreshold vibratory noise provided by the devices cannot fully mitigate their encumbrance and weight, making the tracking task more challenging compared to performing it without any devices. This is evident as the control group outperformed the three groups using the devices. Additionally, at each subthreshold level, the TouchDiver and QuestPro controllers performed better than the VoiceCoil mounted on the gravity compensator, indicating

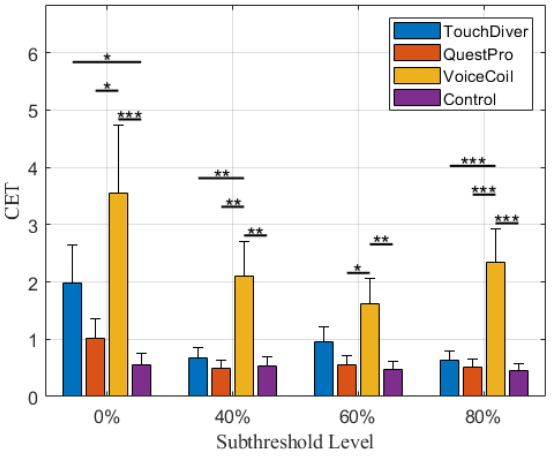

FIGURE 5. Results of the statistical analysis. CET values are reported for each group divided by subthreshold level. For each group, statistical significant differences between subthreshold levels are reported on top of the bins (*: $p < 0.05$, **: $p < 0.01$, ***: $p < 0.001$).

that the latter may have restricted the users' range of motion despite compensating for the arm's weight. To better analysis this phenomenon, we decided to evaluate how varying the subthreshold level influences performance in following a trajectory

We investigated the simple main effect of subthreshold on CET within each group by running a one-way model. The simple main effect of subthreshold levels was significant ($p < 0.05$) for each group except for the control group, which confirms the validity of our experimental protocol as no subthreshold vibratory noise was provided to the control group.

3) INTERACTION BETWEEN CET AND DEVICE

The second analysis involved the interaction between the exploited device and the obtained CET values. Multiple pairwise comparison through EMMs method were conducted, to determine how subthreshold vibratory noise levels impact the performance of the three groups using devices. CET scores were statistically significantly different in the following conditions ($p < 0.05$):

- ***Group 1 - TouchDiver:*** $I_{40\%}$, $I_{60\%}$, $I_{80\%}$ performed better than $I_{0\%}$. $I_{40\%}$ and $I_{80\%}$ performed better than $I_{60\%}$;
- ***Group 2 - QuestPro:*** $I_{40\%}$, $I_{60\%}$ and $I_{80\%}$ performed better than $I_{0\%}$;
- ***Group 3 - VoiceCoil:*** $I_{40\%}$ and $I_{60\%}$ performed better than $I_{0\%}$. $I_{60\%}$ performed better than $I_{80\%}$;

Values of CET for each group divided by subthreshold are reported in Tab. 1, and depicted in Fig. 6 together with the corresponding statistical significant differences. The test assessed that the presence of subthreshold vibratory noise improves the ability to follow a 3D trajectory when users perform the tracking task using a hand-held device, regardless of the specific intensity. Moreover, these results suggest that there is an optimal subthreshold level that may vary

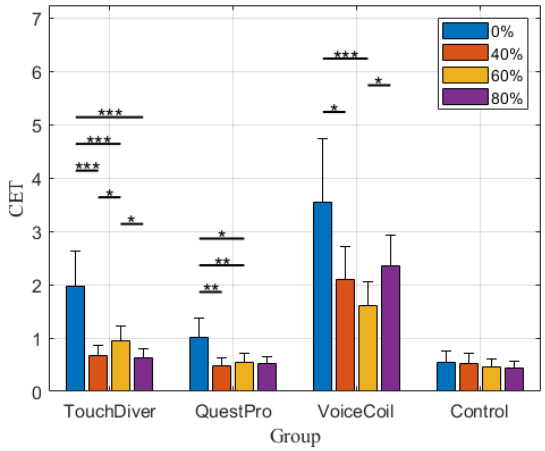

FIGURE 6. Results of the statistical analysis. CET values are reported for each subthreshold divided by the device. Statistical significant differences between groups within the same subthreshold level are reported on top of the bins (*: $p < 0.05$, **: $p < 0.01$, ***: $p < 0.001$).

TABLE 1. Experimental results. The table reports for each group the average trial CET among the subjects for each subthreshold level. The same values are visually reported in Fig. 5 and Fig. 6 together with the statistical significant differences. Values of the last row are highlighted in gray to stress that subjects in the Control group had no haptic interfaces, hence no SR was provided. It is worth noting that the division into four distinct subthreshold level was undertaken in a pseudo-randomized order only for the sake of comparisons, since no stimuli were provided to the participants.

CET				
	Subtreshold Level			
Group	0%	40%	60%	80%
TouchDiver	1.97 ± 0.66	0.67 ± 0.20	0.95 ± 0.26	0.63 ± 0.16
QuestPro	1.00 ± 0.35	0.48 ± 0.15	0.55 ± 0.16	0.52 ± 0.14
VoiceCoil	3.55 ± 1.19	2.10 ± 0.61	1.62 ± 0.44	2.34 ± 0.58
Control	0.55 ± 0.21	0.53 ± 0.17	0.47 ± 0.14	0.44 ± 0.12

depending on the device used. For instance, while users with the TouchDiver performed better at the $I_{80\%}$ level compared to the $I_{60\%}$ level, users with the VoiceCoil device showed the opposite result. Additionally, the obtained CET values exhibit a U-shaped pattern, characteristic of the SR phenomenon. For example, as illustrated in Fig. 6, CET values for the QuestPro and VoiceCoil groups decrease as the subthreshold noise level increases to a certain point, but then start to increase. This could indicate the optimal subthreshold noise level for enhancing users performance [38].

B. TRANSLATIONAL PATH ERROR (TPE)

1) PRELIMINARY STATISTICAL ANALYSIS

Similarly to what we have done with the CETs, we statistically analyzed performance using TPE as a metric. The mean TPEs obtained were not initially normally distributed, as assessed by Shapiro-Wilk's test, thus they were normalized using a logaritmic transformation. After that, all the data were normally distributed ($p > 0.05$). We removed 3 outliers from the analysis. The removal not affect the results, as assessed by comparing the results with and without the outliers. There was homogeneity of variances for 8 over 12 groups, as confirmed by Levene's test for equality of variances ($p > 0.05$). The group sample sizes were approximately equal, and the ratio of the largest group variance (1.3) to the smallest group variance (0.66) was 1.97, thus less than 3. Such condition allowed to run the three-way mixed ANOVA anyway because this test is robust to heterogeneity of variance in these circumstances [37].

For the three-way interaction effect, Mauchly's test of sphericity indicated that the assumption of sphericity was violated. Consequently, a Greenhouse-Geisser correction was applied. The test revealed no statistically significant three-way interaction between device, trajectory and subthreshold, $F(13.43, 152.26) = 1.29$, $p = 0.222$. However, a statistically significant two-way interaction was assessed between subthreshold and device, $F(6.8, 77.05) = 2.268$, $p = 0.039$. Conversely, there were no statistically significant two-way interactions between trajectory and device ($F(5.53, 62.66) = 0.576$, $p = 0.734$), and trajectory and subthreshold ($F(4.48, 152, 26) = 1.017$, $p = 0.405$). Even though trajectory showed no statistically significant interaction with device and subthreshold, its main effect revealed a statistically significant difference in CET values between the different trajectories proposed ($F(1.84, 62.66) = 32.158$, $p < 0.001$). This confirms that, although different trajectories influence TPE due to varying difficulty levels, the impact of subthreshold vibratory noise and device on tracking precision is independent of the difficulty of the trajectory.

2) INTERACTION BETWEEN TPE AND SUBTHRESHOLD

Starting from the results of the preparatory analysis, we decided to investigate the interaction between subthreshold and TPE considering the effect of the device. This was done by further exploring the two-way interaction showed by the ANOVA. The simple main effect of device on CET was investigated at each subthreshold level by running a one-way model. The results demonstrated that the simple main effect of the device was significant for each subthreshold level ($p < 0.001$). Multiple pairwise comparison through estimated marginal means method were conducted, to determine which device effects were statistically significant at each subthreshold level. More in detail, scored CETs were statistically significantly different in the following conditions ($p < 0.05$):

- $I_{0\%}$: Control outperform VoiceCoil and TouchDiver. QuestPro is better than VoiceCoil;
- $I_{40\%}$: TouchDiver, QuestPro, and Control are better than VoiceCoil;
- $I_{60\%}$: Control is better than VoiceCoil;
- $I_{80\%}$: TouchDiver, QuestPro, and Control are better than VoiceCoil.

Fig. 7 visually summarizes the statistical differences between groups within each subthreshold. We can observe that these

results align with those obtained from the CET metric, indicating that the subthreshold vibratory noise provided by the devices cannot counteract their encumbrance and weight. The tracking task with the devices was more challenging compared to performing it without any of them, resulting in poorer tracking precision for users utilizing the latter. This is evident as the control group outperformed the three groups using the devices. Additionally, at each subthreshold level, the TouchDiver and QuestPro controllers performed better than the VoiceCoil mounted on the gravity compensator, confirming that the latter restricted the users' range of motion despite compensating for the arm's weight, resulting in worse tracking precision. An exception is the $I_{60\%}$ level, where the three devices are no more comparable in terms of tracking precision. This suggests that the $I_{60\%}$ level could be an optimal noise level to make a particularly limiting device comparable with a more comfortable one. As a further investigation, we decided to evaluate how varying the subthreshold level influences tracking precision in following a trajectory.

3) INTERACTION BETWEEN TPE AND DEVICE

As a final analysis on the interactions with TPE, we investigated the simple main effect of subthreshold on TPE within each group by running a one-way model. The simple main effect of subthreshold levels was significant ($p < 0.05$) only in the group which used the TouchDiver device. Multiple pairwise comparison through estimated marginal means were conducted, to determine how subthreshold vibratory noise levels impact the performance of the three groups using devices. Specifically, TPE scores were statistically significantly different in the following conditions ($p < 0.05$):

Group 1 - TouchDiver: $I_{40\%}$, $I_{60\%}$, $I_{80\%}$ performed better than $I_{0\%}$. $I_{40\%}$ and $I_{80\%}$ performed better than $I_{60\%}$;

TPE values for each group divided by subthreshold are reported in Tab. 2, and depicted in Fig. 8 together with the corresponding statistical significant differences. The test results for *Group1* were identical to those obtained for the CET metric, suggesting that the performance improvement is effectively due to better tracking precision, resulting in a lower translational path error. In this case, the effect of the subthreshold vibratory noise was significant only for the TouchDiver device. This could suggests that SR is able to improve user tracking precision only when the noise source is near the hand point being moved to follow the trajectory. This is supported also by the fact that the TouchDiver device applied the subthreshold noise directly to the users' index finger, where also the tracking cursor was located (Fig. 4a).

C. TRIAL TIME (TT)

1) PRELIMINARY STATISTICAL ANALYSIS

The mean TTs obtained were not initially normally distributed, as assessed by Shapiro-Wilk's test, thus they were normalized using a logaritmic transformation. After that, all the data were normally distributed ($p > 0.05$). There were 21 outliers, as confirmed by boxplot inspection.

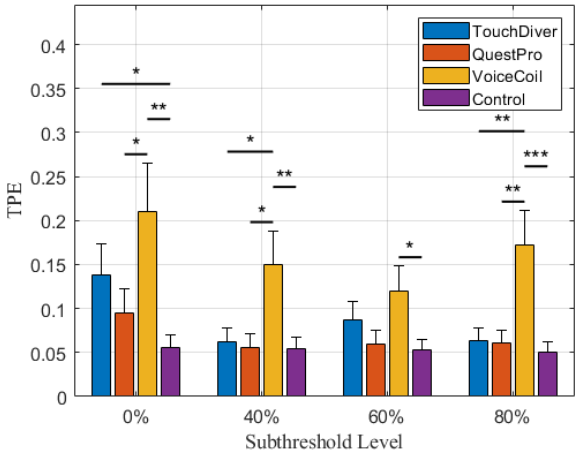

FIGURE 7. Results of the statistical analysis. TPE values are reported for each group divided by subthreshold level. For each group, statistical significant differences between subthreshold levels are reported on top of the bins (*: $p < 0.05$, **: $p < 0.01$, ***: $p < 0.001$).

TABLE 2. Experimental results. The table reports for each group the average trial TPE among the subjects for each subthreshold level. The same values are visually reported in Fig. 7 and Fig. 8 together with the statistical significant differences. Values of the last row are highlighted in gray to stress that subjects in the Control group had no haptic interfaces, hence no SR was provided. It is worth noting that the division into four distinct subthreshold level was undertaken in a pseudo-randomized order only for the sake of comparisons, since no stimuli were provided to the participants.

	TPE			
	Subtreshold Level			
Group	0%	40%	60%	80%
TouchDiver	0.14 ± 0.04	0.06 ± 0.01	0.09 ± 0.02	0.06 ± 0.01
QuestPro	0.09 ± 0.03	0.05 ± 0.01	0.06 ± 0.01	0.06 ± 0.01
VoiceCoil	0.21 ± 0.05	0.15 ± 0.04	0.12 ± 0.03	0.17 ± 0.03
Control	0.056 ± 0.01	0.05 ± 0.01	0.05 ± 0.01	0.05 ± 0.01

We removed 6 outliers from the analysis while keeping the other ones, because they did not materially affect the results, as assessed by comparing the results with and without the outliers. There was homogeneity of variances all the 12 groups, as confirmed by Levene's test for equality of variances ($p > 0.05$). For the three-way interaction effect, Mauchly's test of sphericity indicated that the assumption of sphericity was violated. Consequently, a Greenhouse-Geisser correction was applied. The test revealed no statistically significant three-way interaction between device, trajectory and subthreshold, $F(12.69, 135.32) = 1.206$, $p = 0.283$. However, a statistically significant two-way interaction was assessed between subthreshold and device, $F(4.76, 50.74) = 14.277$, $p < 0.001$. Conversely, there were no statistically significant two-way interactions between trajectory and device ($F(4.68, 49.97) = 1.585$, $p = 0.185$), and trajectory and subthreshold ($F(4.23, 135.32) = 0.115$, $p = 0.98$). Even though trajectory showed no statistically significant interaction with device and subthreshold, its main effect

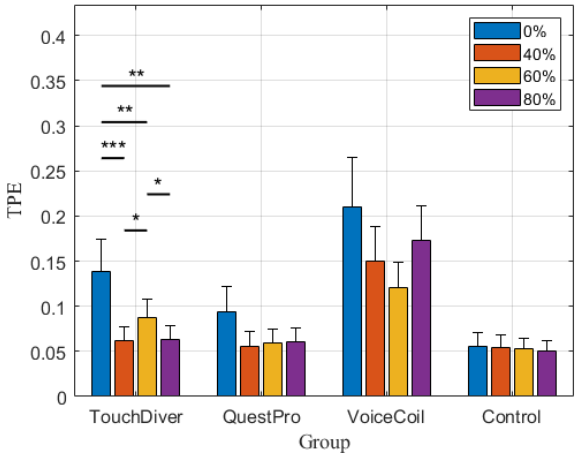

FIGURE 8. Results of the statistical analysis. TPE values are reported for each subthreshold divided by the device. Statistical significant differences between groups within the same subthreshold level are reported on top of the bins (*: $p < 0.05$, **: $p < 0.01$, ***: $p < 0.001$).

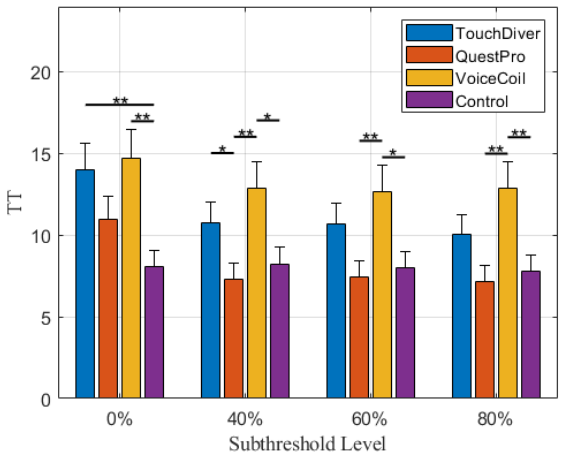

FIGURE 9. Results of the statistical analysis. TT values are reported for each group divided by subthreshold level. For each group, statistical significant differences between subthreshold levels are reported on top of the bins (*: $p < 0.05$, **: $p < 0.01$, ***: $p < 0.001$).

revealed a statistically significant difference in CET values between the different trajectories proposed ($F(1.56, 49.97) = 121.944$, $p < 0.001$). This confirms that, although different trajectories influence TT due to varying difficulty levels, the impact of subthreshold vibratory noise and device on trial time is independent of the difficulty of the trajectory.

2) INTERACTION BETWEEN TT AND SUBTHRESHOLD

A more thorough investigation into the interaction between subthreshold and TT considering the effect of the device was conducted. This was done by further exploring the two-way interaction showed by the ANOVA. The simple main effect of device on TT was investigated at each subthreshold level by running a one-way model. The results demonstrated that the simple main effect of the device was significant for each subthreshold level ($p < 0.001$). Multiple pairwise comparison through estimated marginal means method were conducted, to determine which device effects were statistically significant at each subthreshold level. More in detail, scored TTs were statistically significantly different in the following conditions ($p < 0.05$):

$I_{0\%}$: Control outperform VoiceCoil and TouchDiver;
$I_{40\%}$: QuestPro, and Control are better than VoiceCoil. QuestPro is better than TouchDiver;
$I_{60\%}$: QuestPro and Control are better than VoiceCoil;
$I_{80\%}$: QuestPro, and Control are better than VoiceCoil.

Fig. 9 visually summarizes the statistical differences between groups within each subthreshold. Also these results slightly differ from those obtained from the CET metric, indicating that the subthreshold vibratory noise provided by the devices cannot counteract their encumbrance and weight. The tracking task with the devices was more challenging compared to performing it without any of them, resulting in slower tracking for users utilizing the latter. This is evident as the control group outperformed the three groups using the devices. Additionally, at each subthreshold level, this time only the QuestPro

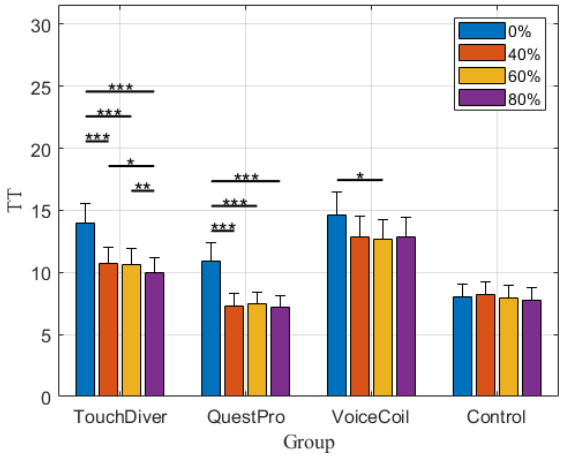

FIGURE 10. Results of the statistical analysis. TT values are reported for each subthreshold divided by the device. Statistical significant differences between groups within the same subthreshold level are reported on top of the bins (*: $p < 0.05$, **: $p < 0.01$, ***: $p < 0.001$).

controllers performed better than the VoiceCoil mounted on the gravity compensator. As subsequent step, we evaluated how varying the subthreshold level influences the time needed to follow a trajectory.

3) INTERACTION BETWEEN TT AND DEVICE

Finally, we investigated the simple main effect of subthreshold on TT within each group by running a one-way model. The simple main effect of subthreshold levels was significant ($p < 0.05$). Multiple pairwise comparison through estimated marginal means method were conducted, to determine how subthreshold vibratory noise levels impact the performance of the three groups using devices. Specifically, CET scores were statistically significantly different in the following conditions ($p < 0.05$):

TABLE 3. Experimental results. The table reports for each group the average Trial Time among the subjects for each subthreshold level. The same values are visually reported in Fig. 9 and Fig. 10 together with the statistical significant differences. Values of the last row are highlighted in gray to stress that subjects in the Control group had no haptic interfaces, hence no SR was provided. It is worth noting that the division into four distinct subthreshold level was undertaken in a pseudo-randomized order only for the sake of comparisons, since no stimuli were provided to the participants.

	TT			
	Subtreshold Level			
Group	0%	40%	60%	80%
TouchDiver	13.96 ± 1.62	10.72 ± 1.28	10.67 ± 1.27	10.01 ± 1.20
QuestPro	10.94 ± 1.42	7.30 ± 0.98	7.43 ± 0.99	7.18 ± 0.96
VoiceCoil	14.66 ± 1.79	12.88 ± 1.62	12.66 ± 1.59	12.84 ± 1.63
Control	8.05 ± 0.98	8.21 ± 1.04	7.97 ± 1.00	7.77 ± 0.98

Group 1 - TouchDiver: $I_{40\%}$, $I_{60\%}$, $I_{80\%}$ performed better than $I_{0\%}$. $I_{80\%}$ performed better than $I_{40\%}$ and $I_{60\%}$;

Group 2 - QuestPro: $I_{40\%}$, $I_{60\%}$ and $I_{80\%}$ performed better than $I_{0\%}$;

Group 3 - VoiceCoil: $I_{60\%}$ performed better than $I_{0\%}$;

TT values for each group divided by subthreshold are reported in Tab. 3, and depicted in Fig. 10 together with the corresponding statistical significant differences. The test assessed that also by evaluating the trial time the presence of subthreshold vibratory noise improves the ability to follow a 3D trajectory when users perform the tracking task using a hand-held device, regardless of the specific intensity in terms of time nedeed to follow a trajectory.

V. CONCLUSION AND FUTURE WORK

This study aimed to investigate the influence of stochastic resonance on the somatosensory system, particularly focusing on hand motion performance. To conduct this investigation, we carried out an experimental study involving 40 participants. We developed a mixed reality environment where participants were tasked with controlling a virtual cursor to track three distinct 3D virtual paths within their surrounding environment. Concurrently, they received subthreshold vibratory white mechanical noise stimulation at the hand through three different haptic interfaces.

The findings from the experimental campaign revealed that users demonstrated enhanced task performance when they were not using any device. This result can be linked to the influence of the weight and ergonomics of the haptic interface on users' precision during the tracking task. Specifically, subjects of the groups TouchDiver and QuestPro had to concurrently account for the weight of the device while executing the task. Meanwhile, subjects of the group VoiceCoil may have experienced a slightly constrained range of motion owing to the presence of the arm support, as in this case the weight was compensated.

On the other hand, it is worth noting that subjects using TouchDiver and QuestPro consistently performed better on the tracking task when the devices applied subthreshold vibratory noise compared to when the same devices were turned off, achieving performance levels comparable to those of the control group. The same result did not hold true for the VoiceCoil group, where the benefits of SR introduced by the mechanical vibration were not substantial enough to result in a significant performance improvement to match the control group. However, in the case of the VoiceCoil, we observed a significant performance improvement when the noise intensity was set at 60% of the subthreshold level. This finding aligns with other studies in the literature, where the SR effect resulted in enhanced performance at this subthreshold percentage [33], [38], [39].

Moreover, by combining the results of the three metrics, we can observe how different vibratory noise levels influence various aspects of a tracking task depending on the device used. For instance, the group using the VoiceCoil showed better performance in terms of CET when the subthreshold noise level was set to $I_{40\%}$ and $I_{60\%}$ compared to when no noise was provided. This indicates that these two thresholds improved performance in terms of the accuracy-speed trade-off. However, when analyzing the simple effect of TT for the same device, only the improvement from the $I_{60\%}$ level was significant, suggesting that only this threshold contributed to a better performance in terms of shorter trial time for following the trajectories. Additionally, by comparing the simple effect of subthreshold within the TouchDiver group, we can see that the $I_{40\%}$ and $I_{80\%}$ levels led to better performance in terms of CET and TPE compared to the $I_{60\%}$ threshold. This indicates that these two thresholds better improve tracking precision while maintaining a good precision-trial time trade-off. However, when looking at the simple effect for TT, the $I_{80\%}$ level was the best for achieving a shorter trial time for the tracking task, showing a smaller TT compared to the $I_{40\%}$ and $I_{60\%}$ levels.

In summary, while subthreshold vibratory noise alone did not improve human hand motion capabilities compared to the bare hand case, as it was unable to overcome the possible drawbacks introduced by the haptic interfaces, it significantly enhanced participants' performance when they were required to use a device for the tracking task. These outcomes represent a noteworthy advancement in the study of the influence of stochastic resonance on human motor abilities, affirming that users demonstrate greater skill and precision in scenarios where device usage is obligatory and SR stimulation is provided. Therefore, it is possible to assert that subthreshold haptic cues have effectively mitigated the performance decline associated with device weight and kinematic constraints. This achievement holds significant promise for enhancing human sensorimotor abilities, particularly in tasks demanding precise hand movements when using handheld devices.

In conclusion, this work establishes the groundwork for asserting that stochastic resonance, in the form of subthreshold vibratory mechanical white noise, has the potential to enhance human hand motion capabilities. This result serves as a foundation for future research, where we will investigate this effect using lightweight and unobtrusive devices strategically

positioned at various points on the hand (including the fingertip, first phalanx, palm, and back of the hand) as well as at the wrist considering various mass and holding styles. These devices will apply vibrations at a subthreshold intensity without impeding or constraining hand movement in any way. This will enable us to comprehensively evaluate whether subthreshold vibratory noise can genuinely improve the absolute precision of human hand movements. Future work will also consider gender and age effects on the perception and effectiveness of subthreshold vibration intensity.

REFERENCES

[1] P. Hänggi, "Stochastic resonance in biology how noise can enhance detection of weak signals and help improve biological information processing," *ChemPhysChem*, vol. 3, no. 3, pp. 285–290, Mar. 2002.

[2] G. P. Harmer, B. R. Davis, and D. Abbott, "A review of stochastic resonance: Circuits and measurement," *IEEE Trans. Instrum. Meas.*, vol. 51, no. 2, pp. 299–309, Apr. 2002.

[3] F. Moss, L. M. Ward, and W. G. Sannita, "Stochastic resonance and sensory information processing: A tutorial and review of application," *Clin. Neurophysiol.*, vol. 115, no. 2, pp. 267–281, 2004.

[4] A. N. Mikhaylov, D. V. Guseinov, A. I. Belov, D. S. Korolev, V. A. Shishmakova, M. N. Koryazhkina, D. O. Filatov, O. N. Gorshkov, D. Maldonado, F. J. Alonso, J. B. Roldán, A. V. Krichigin, N. V. Agudov, A. A. Dubkov, A. Carollo, and B. Spagnolo, "Stochastic resonance in a metal-oxide memristive device," *Chaos, Solitons Fractals*, vol. 144, Mar. 2021, Art. no. 110723.

[5] W. Zhang, A. Song, H. Zeng, B. Xu, and M. Miao, "The effects of bilateral phase-dependent closed-loop vibration stimulation with motor imagery paradigm," *IEEE Trans. Neural Syst. Rehabil. Eng.*, vol. 30, pp. 2732–2742, 2022.

[6] W. Zhang, A. Song, H. Zeng, B. Xu, and M. Miao, "Closed-loop phase-dependent vibration stimulation improves motor imagery-based brain-computer interface performance," *Frontiers Neurosci.*, vol. 15, Jan. 2021, Art. no. 638638.

[7] F. Monifi, J. Zhang, S. K. Özdemir, B. Peng, Y.-X. Liu, F. Bo, F. Nori, and L. Yang, "Optomechanically induced stochastic resonance and chaos transfer between optical fields," *Nature Photon.*, vol. 10, no. 6, pp. 399–405, Jun. 2016.

[8] Z. Qiao and X. Shu, "Coupled neurons with multi-objective optimization benefit incipient fault identification of machinery," *Chaos, Solitons Fractals*, vol. 145, Apr. 2021, Art. no. 110813.

[9] S. Mitaim and B. Kosko, "Adaptive stochastic resonance in noisy neurons based on mutual information," *IEEE Trans. Neural Netw.*, vol. 15, no. 6, pp. 1526–1540, Nov. 2004.

[10] S. Blanchard, D. Rousseau, and F. Chapeau-Blondeau, "Noise enhancement of signal transduction by parallel arrays of nonlinear neurons with threshold and saturation," *Neurocomputing*, vol. 71, nos. 1–3, pp. 333–341, Dec. 2007.

[11] O. White, J. Babič, C. Trenado, L. Johannsen, and N. Goswami, "The promise of stochastic resonance in falls prevention," *Frontiers Physiol.*, vol. 9, p. 1865, Jan. 2019.

[12] C. Trenado, A. Mikulić, E. Manjarrez, I. Mendez-Balbuena, J. Schulte-Mönting, F. Huethe, M.-C. Hepp-Reymond, and R. Kristeva, "Broad-band Gaussian noise is most effective in improving motor performance and is most pleasant," *Frontiers Hum. Neurosci.*, vol. 8, p. 22, Feb. 2014.

[13] C. M. Germer, A. Del Vecchio, F. Negro, D. Farina, and L. A. Elias, "Neurophysiological correlates of force control improvement induced by sinusoidal vibrotactile stimulation," *J. Neural Eng.*, vol. 17, no. 1, Jan. 2020, Art. no. 016043.

[14] B. Xiao, L. Liu, L. Chen, X. Wang, X. Zhang, X. Liu, W. Hou, and X. Wu, "Neuro-muscular responses adaptation to dynamic changes in grip strength," *IEEE Trans. Neural Syst. Rehabil. Eng.*, vol. 32, pp. 3189–3198, 2024.

[15] J. J. Collins, A. A. Priplata, D. C. Gravelle, J. Niemi, J. Harry, and L. A. Lipsitz, "Noise-enhanced human sensorimotor function," *IEEE Eng. Med. Biol. Mag.*, vol. 22, no. 2, pp. 76–83, Mar. 2003.

[16] R. Dickstein and Y. Laufer, "Light touch and center of mass stability during treadmill locomotion," *Gait Posture*, vol. 20, no. 1, pp. 41–47, Aug. 2004.

[17] L. Johannsen, A. M. Wing, and V. Hatzitaki, "Effects of maintaining touch contact on predictive and reactive balance," *J. Neurophysiol.*, vol. 97, no. 4, pp. 2686–2695, Apr. 2007.

[18] F. H. Magalhães and A. F. Kohn, "Vibratory noise to the fingertip enhances balance improvement associated with light touch," *Exp. Brain Res.*, vol. 209, no. 1, pp. 139–151, Mar. 2011.

[19] T. Kimura, M. Kouzaki, K. Masani, and T. Moritani, "Unperceivable noise to active light touch effects on fast postural sway," *Neurosci. Lett.*, vol. 506, no. 1, pp. 100–103, Jan. 2012.

[20] C. Trenado, I. Mendez-Balbuena, E. Manjarrez, F. Huethe, J. Schulte-Mönting, B. Feige, M.-C. Hepp-Reymond, and R. Kristeva, "Enhanced corticomuscular coherence by external stochastic noise," *Frontiers Hum. Neurosci.*, vol. 8, p. 325, May 2014.

[21] S. Lee, D. J. Kim, D. Svenkeson, G. Parras, M. M. K. Oishi, and M. J. McKeown, "Multifaceted effects of noisy galvanic vestibular stimulation on manual tracking behavior in Parkinson's disease," *Frontiers Syst. Neurosci.*, vol. 9, p. 5, Feb. 2015.

[22] S. Pal, S. M. Rosengren, and J. G. Colebatch, "Stochastic galvanic vestibular stimulation produces a small reduction in sway in Parkinson's disease," *J. Vestibular Res.*, vol. 19, nos. 3–4, pp. 137–142, Apr. 2010.

[23] I. Mendez-Balbuena, E. Manjarrez, J. Schulte-Mönting, F. Huethe, J. A. Tapia, M.-C. Hepp-Reymond, and R. Kristeva, "Improved sensorimotor performance via stochastic resonance," *J. Neurosci.*, vol. 32, no. 36, pp. 12612–12618, Sep. 2012.

[24] R. Hoskins, J. Wang, and C. G. L. Cao, "Use of stochastic resonance methods for improving laparoscopic surgery performance," *Surgical Endoscopy*, vol. 30, no. 10, pp. 4214–4219, Oct. 2016.

[25] C. Wells, L. M. Ward, R. Chua, and J. T. Inglis, "Touch noise increases vibrotactile sensitivity in old and young," *Psychol. Sci.*, vol. 16, no. 4, pp. 313–320, Apr. 2005.

[26] M. Bagherzadeh Cham, M. A. Mohseni-Bandpei, M. Bahramizadeh, S. Kalbasi, and A. Biglarian, "The clinical and biomechanical effects of subthreshold random noise on the plantar surface of the foot in diabetic patients and elder people: A systematic review," *Prosthetics Orthotics Int.*, vol. 40, no. 6, pp. 658–667, 2016.

[27] S. Nobusako, M. Osumi, A. Matsuo, T. Fukuchi, A. Nakai, T. Zama, S. Shimada, and S. Morioka, "Stochastic resonance improves visuomotor temporal integration in healthy young adults," *PLoS ONE*, vol. 13, no. 12, Dec. 2018, Art. no. e0209382.

[28] F. Duan, L. Duan, F. Chapeau-Blondeau, Y. Ren, and D. Abbott, "Binary signal transmission in nonlinear sensors: Stochastic resonance and human hand balance," *IEEE Instrum. Meas. Mag.*, vol. 23, no. 1, pp. 44–49, Feb. 2020.

[29] Y. Kurita, Y. Sueda, T. Ishikawa, M. Hattori, H. Sawada, H. Egi, H. Ohdan, J. Ueda, and T. Tsuji, "Surgical grasping forceps with enhanced sensorimotor capability via the stochastic resonance effect," *IEEE/ASME Trans. Mechatronics*, vol. 21, no. 6, pp. 2624–2634, Dec. 2016.

[30] C. C. A. M. Gielen, T. M. H. Dijkstra, I. J. Roozen, and J. Welten, "Coordination of gaze and hand movements for tracking and tracing in 3D," *Cortex*, vol. 45, no. 3, pp. 340–355, Mar. 2009.

[31] R. Bayramova, I. Valori, P. E. McKenna-Plumley, C. Z. Callegher, and T. Farroni, "The role of vision and proprioception in self-motion encoding: An immersive virtual reality study," *Attention, Perception, Psychophys.*, vol. 83, no. 7, pp. 2865–2878, Oct. 2021.

[32] T. N. Cornsweet, "The staircase-method in psychophysics," *Amer. J. Psychol.*, vol. 75, no. 3, pp. 485–491, Sep. 1962.

[33] S. Ikemura, T. Endo, and F. Matsuno, "Multiple remote vibrotactile noises improve tactile sensitivity of the fingertip via stochastic resonance," *IEEE Access*, vol. 9, pp. 17011–17019, 2021.

[34] M. M. Coad, A. M. Okamura, S. Wren, Y. Mintz, T. S. Lendvay, A. M. Jarc, and I. Nisky, "Training in divergent and convergent force fields during 6-DOF teleoperation with a robot-assisted surgical system," in *Proc. IEEE World Haptics Conf. (WHC)*, Jun. 2017, pp. 195–200.

[35] P. M. Fitts, "The information capacity of the human motor system in controlling the amplitude of movement," *J. Experim. Psychol.*, vol. 47, no. 6, pp. 381–391, 1954.

[36] J. Fowler, L. Cohen, and P. Jarvis, *Practical Statistics for Field Biology*. Hoboken, NJ, USA: Wiley, 2013.

[37] W. T. Coombs, J. Algina, and D. O. Oltman, "Univariate and multivariate omnibus hypothesis tests selected to control type i error rates when population variances are not necessarily equal," *Rev. Educ. Res.*, vol. 66, no. 2, pp. 137–179, 1996.

[38] K. Chamnongthai, T. Endo, F. Matsuno, K. Fujimoto, and M. Kosaka, "Two-dimensional fingertip force training with improved haptic sensation via stochastic resonance," *IEEE Trans. Hum.-Mach. Syst.*, vol. 50, no. 6, pp. 593–603, Dec. 2020.
[39] N. J. Seo, K. Lakshminarayanan, L. Bonilha, A. W. Lauer, and B. D. Schmit, "Effect of imperceptible vibratory noise applied to wrist skin on fingertip touch evoked potentials—An EEG study," *Physiological Rep.*, vol. 3, no. 11, Nov. 2015, Art. no. e12624.

MICHELE POMPILIO (Member, IEEE) received the B.S. and M.S. degrees in computer and automation engineering from the Politecnico di Torino, in 2019 and 2022, respectively. He is currently pursuing the Ph.D. degree with the Department of Information Engineering and Mathematics, University of Siena. He is also a Ph.D. Fellow with the Humanoids and Human Centered Mechatronics Department, Istituto Italiano di Tecnologia (IIT). His research interests include wearable haptics and human centered robotics.

NICOLE D'AURIZIO (Member, IEEE) received the M.Sc. degree (cum laude) in computer and automation engineering from the University of Siena, in 2017 and 2019, respectively, and the Ph.D. degree in automatic control and robotics from the Department of Information Engineering and Mathematics, University of Siena, in 2023. She was a Ph.D. Fellow with the Department of Advanced Robotics, Istituto Italiano di Tecnologia (IIT), from 2019 to 2022. She is currently an Assistant Professor with the Department of Information Engineering and Mathematics, University of Siena, and a Research Affiliate with the Istituto Italiano di Tecnologia. Her research interests include haptics and robotics, focusing on wearable and affective haptics and human centered robotics.

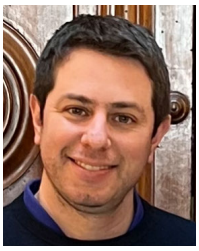

TOMMASO LISINI BALDI (Member, IEEE) received the M.Sc. degree (cum laude) in computer and automation engineering and the Ph.D. degree in robotic and automation from the Department of Information Engineering and Mathematics, University of Siena, Siena, Italy, in 2014 and 2018, respectively. He was a Ph.D. Fellow with the Department of Advanced Robotics, Istituto Italiano di Tecnologia, from 2014 to 2017. Currently, he is an Assistant Professor with the University of Siena and a Research Affiliate with the Istituto Italiano di Tecnologia. His research interests include robotics and haptics focusing on human–robot collaboration, haptic feedback, wearable technologies, and motion tracking with inertial sensors.

GIONATA SALVIETTI (Senior Member, IEEE) received the master's degree in computer engineering and the Ph.D. degree in information engineering from the University of Siena, Siena, Italy, in 2009 and 2012, respectively. In 2012, he was a Visiting Researcher with the DLR Institute of Robotics and Mechatronics, Weblling, Germany. From 2012 to 2015, he was a Postdoctoral Researcher with Italian Institute of Technology, Genoa, Italy. He is currently an Associate Professor with the Department of Information Engineering and Mathematics, University of Siena, and an Affiliated Researcher with Italian Institute of Technology. His research interests include collaborative robotics, assistive devices, and haptics.

SIMONE ROSSI received the M.D. degree from the University of Firenze, in 1987, the degree in neurophysiopathlogy from the University of Genova, in 1990, the Ph.D. degree in pathophysiology of nervous functions, in 1996, and the degree in neurology from the University of Siena, Siena, Italy, in 1999. He is currently a Neurologist and a Neurophysiologist and also the Director of the Brain Investigation and Neuromodulation Laboratory (Si-BIN Laboratory), Department of Neuroscience, Neurology and Clinical Neurophysiology Unit, University of Siena, where he is also leading the Parkinson's Disease and movement disorders clinical activity. He is also the President of Italian Society of Psychophysiology (SIPF).

DOMENICO PRATTICHIZZO (Fellow, IEEE) received the M.S. degree in electronics engineering and the Ph.D. degree in robotics and automation from the University of Pisa, Pisa, Italy, in 1991 and 1995, respectively. He is currently a Professor in robotics with the University of Siena, Siena, Italy. Since 2009, he has been a Scientific Consultant with the Istituto Italiano di Tecnoloogia, Genoa, Italy. In 1994, he was a Visiting Scientist with the MIT AI Laboratory. He has authored more than 200 articles in his research fields. His main research interests include haptics, grasping, visual servoing, and mobile robotics.

Open Access funding provided by 'Università degli Studi di Siena' within the CRUI CARE Agreement